ENGINEERING AND GINNING

Multi-path Interference Mitigation for Cotton Bale Microwave Moisture Sensing

Mathew G. Pelletier

ABSTRACT

Previous research indicated that the effects of multi-path interference on a microwave cotton moisture sensor are significant enough to force a completely new calibration for each and every installation, which is an expensive and time-consuming task. This research was conducted to determine if a system could be designed that would be impervious to multi-path interference. The feasibility of using swept frequency modulation for isolation of the direct free-space signal from the multi-path interference signals was examined through a simulation analysis. The analysis focuses on near range reflectors that are typical in cotton gin applications as opposed to far range reflectors that are common in the telecommunications industry. The results of the analysis indicate the proposed technique provides a 37 dB improvement for multi-path rejection over current techniques.

Optimal control of lint moisture in cotton gins has many advantages from reduced wear on bale press machinery, to improved lint fiber quality, to higher production throughput with higher economic return on the finished product through improved quality control. In order to achieve the optimal control, many of the required sensors are either not available or are very expensive. This research is the continuation of work being conducted to design a low cost, non-contact, free space, microwave moisture sensor to sense packaged cotton bale moisture.

Previous research has shown that the microwave permittivity is directly related to the moisture content and density (Kraszewski, 1988; Kraszewski et al., 1996; Nelson et al., 2000; Trabelsi et al., 2001). Research by Pelletier (2004) has shown the microwave signal through the cotton bale is distorted by multi-path interference (Fig. 1), and multi-path interference

M. G. Pelletier, Agricultural Research Service, United States Department of Agriculture, Route 3, Box 215, Lubbock, TX 79401
mpelletier@lbk.ars.usda.gov

affects the measured permittivity so that both the slope and the intercept of the material being tested are affected during the calibration. The distortion of the permittivity measurement due to the influence of multi-path interference required the microwave sensor to be calibrated on site (Pelletier, 2004). This calibration process is an expensive and time consuming task. An alternative device that would remove or avoid the multi-path influence would lower the end-cost to the consumer. This research explores a novel modulation technique for dielectric sensing with the hope that it will provide a robust rejection of multi-path interference. A system of this type would be advantageous because the known cotton permitivities could then be used to calibrate the system at the manufacturer's factory rather than in a field. This would reduce the installation cost by removing the expensive and time consuming calibration process.
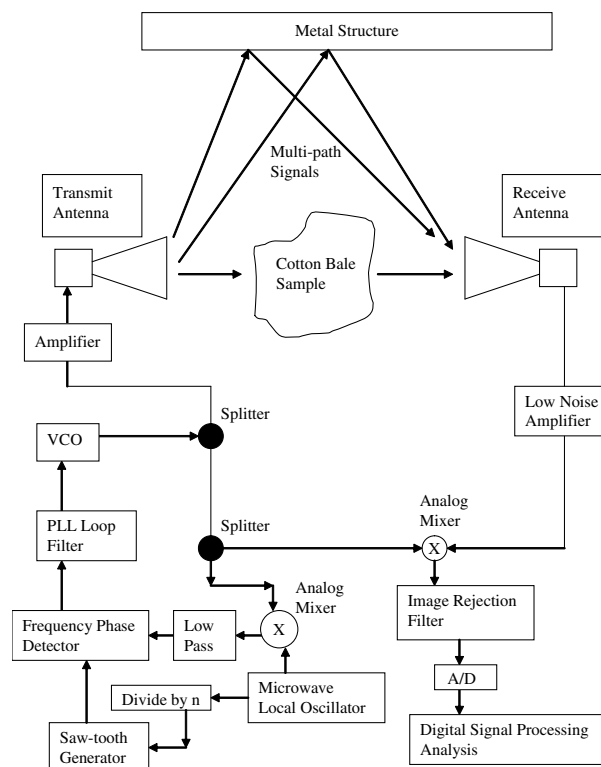

Figure 1: Schematic layout of the microwave cotton bale moisture sensor with multi-path interference. VCO = voltage-controlled oscillator, A/D = analog to digital converter, PPL = phase-locked loop.

This study focused on one type of modulation technique to determine if the technique would provide a system that is tolerant of multi-path interference without destroying the permittivity information contained within the transmitted microwave signal.

In the transmission of microwave energy, a large portion of the signal being transmitted occurs in side lobes. The amount is dependant on the type and forward gain of the antenna. In practice, microwave horns are typically used; however, even with a horn a significant amount of energy is not directed through the 10 degree aperture of interest, leaving the rest of the energy available to propagate out the side and the back of the transmitting antenna in a direction away from the target of the receiving antenna (Cheng, 1992; Balanis, 1982). In the interest of reducing the effects of these spurious emissions, it has become common practice in research applications to improve the front to back ratio through the addition of focusing lenses (Nelson et al., 2000). Given the high cost of focusing microwave horn antennas, this solution is less than desirable for a commercial device.

In addition to the normal off-direction radiation created by the horn antennas, even more energy is reflected off the front face of the cotton bale, due to the impedance miss-match between free-space and the solid cotton bale (Pozar, 1998). It is the combination of the off-axis energy from the horn coupled with the energy reflected off the front edge of the cotton bale that provides the majority of energy for the multi-path interference. Additionally, in most field applications in cotton gins, the units operate within a metal building with metal floors and lots of metal machinery, so radiation that is not directed through the cotton bale will likely become available for multi-path interference. Because of the total number of reflecting surfaces inside a cotton gin, a large number of multi-path interfering signals are likely to be received along with the direct-path signal. This combination of the variously delayed multi-path signals along with the direct-path signal results in the reception of a series of sinusoids of the same frequency but with altered phases and magnitudes.

Multi-path interference is a term commonly used in the telecommunications industry for the situation in which microwave energy received in a direct path is combined with longer path microwave energy that has been delayed by reflecting off neighboring reflectors (Lee and Miller, 1998; Stremler, 1992). Since this reflected energy takes a longer path to reach the antenna, it is out of phase and typically has a smaller amplitude than the direct path energy. This energy typically combines out of phase with the direct path energy leading to reduced signal strength due to destructive signal combination. This phenomenon is well known and numerous modulation schemes have been devised to mitigate this effect (Lee and Miller, 1998). Perhaps the best known technique is the code-division-multiple-access (CDMA) system used in the cellular phone industry. This technique is a spread-spectrum phase modulation scheme that relies on spreading the signal over a very wide frequency bandwidth, and then using a low frequency pseudo-random-noise (PN) chipping signal, it is combined with the desired digital signal. This combined signal is then used to modulate a high-frequency microwave carrier. Upon reception at the receiving antenna, the PN vector is used to demodulate the received carrier. This system works extremely well at removing multi-path interference, because it uses the redundancy of the low frequency PN signal to reject the spurious multi-path signals impinging upon the receiving antenna, thereby adding a significant amount of processing gain (Lee and Miller, 1998).

Unfortunately, for microwave moisture sensing, the standard technique relies on the resolution provided by the unmodulated carrier signal with a frequency greater than 1.5 GHz, so the spread spectrum technique cannot be used with today's technology, because a digital synthesizer that can operate above 400MHz has not been developed. When digital synthesizers that operate above 2-10 GHz become available, a system can be designed to use these techniques in microwave moisture sensing. In lieu of direct utilization, concepts and ideas from this field can be modified and adopted for gin applications. This investigation is a feasibility study to explore a new technique with the goal of providing the accuracy of the continuous wave measurement, while maintaining a significant degree of multi-path rejection. The analysis will be conducted through a simulation study.

MATERIALS AND METHODS

Equation development. In developing a new technique to deal with the multi-path interference issues that arise during microwave moisture measurements, analysis of the combination of the direct-path signal coupled with the multi-path interference provides a basis for further development and insight

into potential solutions. In the telecommunication industry, two or more delayed versions of the direct-path signal, each with a reduced magnitude that is typically much less than one, are combined with the direct-path signal to form a composite received signal is the typical model for multi-path interference (Stremler, 1992). The reduction in magnitude is allowed because it is representative of the real-world phenomenon. In mathematical terms, this signal combination is illustrated as follows:

$$S(t) = A_0 \cdot s(t) + A_1 \cdot s(t + \tau_1) + A_2 \cdot s(t + \tau_2) +$$
$$A_3 \cdot s(t + \tau_3) + \ldots + A_n \cdot s(t + \tau_n) \quad \text{(Eq. 1)}$$

where, $S(t)$ = the received signal as a function of time; $A_0 \cdot s(t)$ = the direct transmitted sinusoidal time-varying signal measured at the detector as a function of time (s); $s(t + \tau_i)$ = the time delayed version of the transmitted signal reflected by cotton lint moisture/air interface (subscript $i = 1$) or multi-path signal (subscript $i = \{2\ldots n\}$; A_{1-n} = signal strength coefficients of multi-path signals).

In typical microwave moisture sensors (Kraszewski, 1988; Kraszewski et al., 1996; Nelson et al., 2000; Trabelsi et al., 2001), the systems use a continuous wave sinusoidal signal to transmit microwaves through the material being tested. The technique measures the relative permittivity of the material through its effect on the transmitted signal (Pozar, 1998). The transmitted signal and the i-th delayed transmitted signal can be represented as detailed in Eqs. 2 and 3a, or equivalently as a phase delayed version of the transmitted signal as shown in Eq. 3b.

$$A_0 \cdot s(t) = A_0 \cdot \sin(\omega \cdot t) \quad \text{(Eq. 2)}$$

$$A_i \cdot s(t + \tau_i) = A_i \cdot \sin(\omega \cdot (t + \tau_i)) \quad \text{(Eq. 3a)}$$

$$A_i \cdot s(t + \theta_i) = A_i \cdot \sin(\omega \cdot t + \theta_i) \quad \text{(Eq. 3b)}$$

where, θ = phase delay of the sinusoidal signal (rads); A_i = amplitude of the i-th signal; $\omega = 2\pi f = 2\pi$ frequency (rads/s).

The information of the complex permittivity of the material is derived by comparing both the reduced amplitude and the phase delay of the received signal with those of the transmitted signal. Combining Eqs. 1 through 3 provides an estimate of the effect of the multi-path interference on the true signal (Eqs. 4 and 5).

$$S(t) = \text{direct Signal} + \text{multi-pathSignal\_1} +$$
$$\text{multi-pathSignal\_2} + \ldots +$$
$$\text{multi-pathSignal\_n} \quad \text{(Eq. 4)}$$

$$S(t) = \sin(\omega \cdot t) + a_c \sin(\omega \cdot t + \theta_c) +$$
$$a_2 \cdot \sin(\omega \cdot t + \theta_2) + a_3 \cdot \sin(\omega \cdot t + \theta_3) +$$
$$\ldots + a_n \cdot \sin(\omega \cdot t + \theta_n) \quad \text{(Eq. 5)}$$

Using basic trigonometry, a sum of sinusoids of the same frequency produces a single sinusoid of that frequency with an altered phase shift and amplitude, so Eq. 5 reduces to Eq. 6.

$$S(t) = B \cdot \sin(\omega \cdot t + \theta_B) \quad \text{(Eq. 6)}$$

where, B = amplitude of the received signal; θ_B = phase of the received signal.

Equation 6 shows that multi-path interference alters the received signal so that the continuous wave permittivity measurement is significantly affected, because the permittivity measurement is based on the measurement of the amplitude and the phase of the transmitted signal. Since the multi-path signal is highly dependant on the geometry of the deployed locale, the unpredictability of the multi-path signal alters the direct-path signal, which is the basis for the microwave permittivity measurement (Pelletier, 2004). It should also be recognized, as illustrated in Eq. 6, the combination of the direct-path signal with the multi-path signals creates a new signal with an altered phase and amplitude. Traditional frequency domain filtering is not an option, so the only other type of filtering that can be used is some form of a time-gating operation, which would cut-off the reception of any signals received after the initial signal is transmitted. Ideally, the signals that would be removed through a time-gating operation, as detailed in Eq. 1, are the signals delayed by τ_i ($i>1$).

There are two methods for time-gating. The first is the direct method of capturing the signal only during a brief window of operation; however, the electronics for direct gating of a GHz plus signal, which allows the direct-path signal to be separated from the multi-path signals that originate from only a few meters away, demands an operational window of less than a nanosecond. In practice, the traditional method for time-gating is to perform a frequency sweep, perform an inverse Fourier transformation to determine the locations of the reflections, sample in the time-domain between these reflections, and then convert back to the frequency domain. Because of the nature of the Fourier transformation, the resolution in the time domain is proportional to the number of samples obtained in the frequency domain and to the bandwidth of the sampling window, so the system must perform a sweep across a significant bandwidth in order to extract qual-

ity time-domain data. Unfortunately, FCC regulations severely restrict the bandwidth for use in commercial equipment, so this technique has limited resolution in a commercial application of the continuous wave permittivity measurement system.

The radar industry uses an alternative form of time-gating that uses a frequency modulated signal, which can be examined after heterodyning the signal down to a lower and more manageable frequency (Peebles, 1998). The goal of a cotton bale moisture measurement system is quite different from the goals of target detection and distance measurement in the radar industry. An analysis of the suitability of this technique is required.

The radio heterodyning signal mixing equation provides a well known model that describes the output of two signals that are combined together in a mixer, and forms a new signal that is a combination of a sum and difference frequency of the two input signals (Stremler, 1992). Mathematically this can be modeled by the multiplication of the two input signals shown in Eq. 7 as follows:

$$Y(t) = \sin(\omega_1 t) \sin(\omega_2 t)$$
$$= 0.5 [\cos(\omega_1 t - \omega_2 t) - \cos(\omega_1 t + \omega_2 t)]$$
$$= 0.5 [\cos(\{\omega_1 - \omega_2\}t) - \cos(\{\omega_1 + \omega_2\}t)] \quad \text{(Eq. 7)}$$

Expanding Eq. 7 to include the phase terms leads to Eqs. 8 and 9.

$$Z(t) = \sin(\omega_1 t + \varphi_1) \sin(\omega_2 t + \varphi_2)$$
$$= 0.5 [\cos(\omega_1 t + \varphi_1 - \omega_2 t - \varphi_2) - \cos(\omega_1 t + \varphi_1 + \omega_2 t + \varphi_2)] \quad \text{(Eq. 8)}$$

and letting

$$\varphi_3 = \varphi_1 - \varphi_2 \text{ and } \varphi_4 = \varphi_1 + \varphi_2$$

then

$$Z(t) = 0.5 [\cos(\{\omega_1 - \omega_2\}t + \varphi_3) - \cos(\{\omega_1 + \omega_2\}t + \varphi_4)] \quad \text{(Eq. 9)}$$

In using a microwave complex permittivity measurement system, it is critical that the phase and the magnitude of the signal are preserved. To examine the potential of a mixer in a permittivity measurement system, the first input signal (Eqs. 7 through 9) will be assigned to the reference signal with unity amplitude and zero phase. The second signal will represent the received direct-path signal with an altered phase and magnitude, as determined by the path length through the material being tested and the material's permittivity. Given this representation, the applied form of Eq. 9 is shown in Eq. 10.

$$Z(t) = \sin(\omega_1 t) A \cdot \sin(\omega_2 t + \varphi_2)$$
$$= 0.5 \cdot A [\cos(\{\omega_1 - \omega_2\}t - \varphi_2) - \cos(\{\omega_1 + \omega_2\}t + \varphi_2)] \quad \text{(Eq. 10)}$$

To remove the upper side-band image, the mixer's output signal is passed through an analog low pass filter, which effectively leaves only the lower side band intact (Eq. 11).

$$Z(t) * Lp(t) = 0.5 \cdot A \cos(\{\omega_1 - \omega_2\}t - \varphi_2) \quad \text{(Eq. 11)}$$

where, $Z(t) * Lp(t)$ = convolution of signal $Z(t)$ with the low pass linear filter $Lp(t)$.

The key point of interest is that both the amplitude and the phase information contained in the direct-path signal number two altered by the cotton is preserved in both the upper-side band ($\omega_1 + \omega_2$) and the lower side band ($\omega_1 - \omega_2$) of the carrier modulated signal. Eq. 11 shows that the mixing operation only translates the signal from one frequency to another without altering the key permittivity information, amplitude, and phase contained in the received direct-path signal after mixing, so the permittivity measurement operation is unaffected by the mixing operation, which is critical to the proposed swept frequency modulation technique. For ease of processing, the system removes one of the side bands through a filtering operation.

System design. The technique under investigation provides the basis for a new system with the goal of shutting out any signal that is delayed beyond the expected direct-path delay. To achieve this goal, the proposed system continuously varies the reference transmission frequency. A block diagram of one possible system that can perform this operation is shown in Figure 1. The primary consequence of this analysis is that the output from the voltage controlled oscillator (VCO) provides a continuously frequency-varying signal, also known as a continuous swept frequency signal. The means for obtaining a stable swept frequency will be determined in subsequent research. The splitter following the VCO is a required element, because it provides the system with both a transmitting signal and an internal reference copy of the transmitted signal. The internal reference signal is combined with the time-delayed received signal, and both signals are inputs. The output of the mixer produces the sum and difference of the frequencies where the frequency variation between the two signals is due to the delay of the transmitted signal as it is propagated through the test material multiplied by the rate of the frequency variation of the swept frequency signal produced by the VCO and its associated control circuit.

The proposed technique of swept frequency permittivity measurement results in the direct-path having a small difference, or delta frequency, while the longer multi-path signals have a larger delta frequency because of the longer circuitous propagation path they take to arrive at the receiving antenna. The magnitude of the frequency difference is determined by the time-delay of the multi-path signals coupled with the frequency excursion of the VCO combined with the VCO control signal's saw-tooth repetition rate. The frequency difference is equal to the transmitted signal's time-delay multiplied by the frequency rate of change of the VCO. In practice, the frequency difference between the direct path and the multi-path components allows for direct removal of the multi-path components by means of a band-pass filter centered on the expected delays of the direct-path signal, thereby removing any multi-path signals that fall outside of this narrow band-pass window.

Additional advantages of this system lie in the inherent ability of the system to measure the phase delay of the direct-path signal as a function of the received frequency difference. This effectively transforms the propagation time delay measurement of the signal from a phase to a frequency difference measurement, which provides the significant advantage of removing the unknown integer-n rollover experienced with a phase measurement. This will be referred to as the phase-ambiguity associated with phase measurement systems. This is illustrated by noting that in the direct phase difference measurement method, the phase difference is limited to +/- 180 degrees before the measurement repeats itself. This technique leads to a phase ambiguity in the processed signal if the total phase delay exceeds a span, across the range of material permittivities of interest, greater than 360 degrees. Conversely, the frequency difference measurement does not suffer from this phase ambiguity issue and can provide a much larger measurement of phase delay than the direct method. This is highly advantageous in some measurement applications where, due to the large depth of the material being tested and the broad range of expected moisture contents, the expected electrical permittivities will cause a phase delay range that exceeds 360 degrees. This leads to a situation where the phase-ambiguity destroys the ability of the system to differentiate short-delay materials (low permittivity) from long-delay materials (high permittivity).

Modeling procedures. The proposed system under investigation provides a continuous frequency swept signal that is transmitted through the cotton bale. This signal is also used as the internal reference signal, which in practice would be obtained by splitting the signal internally and directing one copy as the reference and the other copy towards the external transmitting antenna. One example of the frequency versus time saw-tooth response of the proposed type of transmission signal is detailed in Figure 2. By comparison, the same signal in the time domain is shown in Figure 3, which illustrates that this is a more complicated signal waveform than the single frequency continuous wave method of traditional permittivity measurement systems.
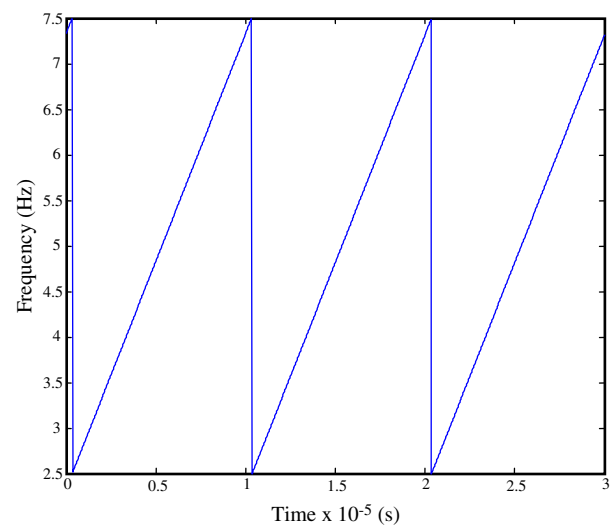

Figure 2: Plot of frequency versus time of the signal that is used to modulate the voltage-controlled oscillator.
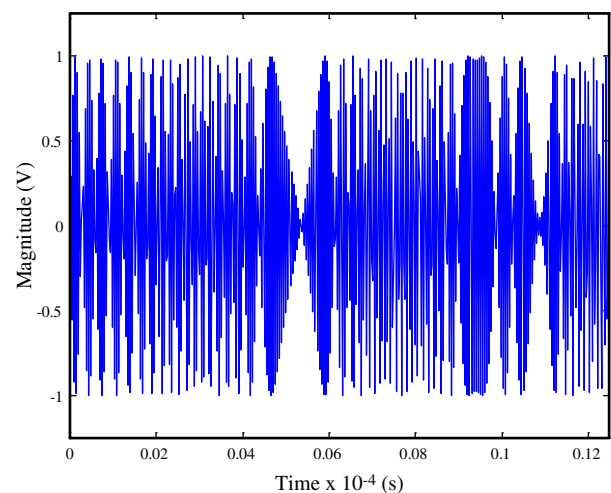

Figure 3: Time-domain plot of the transmitted signal.

If the system is expanded to include the multi-path signals, as discussed previously, a transmitted signal in a multi-path environment will propagate out in multiple directions and take different paths to the receiving antenna, because of the reflection off the neighboring metal clad surfaces. Since each of these multi-path propagation paths are of different lengths, the receiving antenna subsequently receives multiple copies of the original signal, all of which arrive at different delayed times. When a continuous frequency-varying signal is transmitted in a multi-path rich environment, it is received along with multiple copies of the transmitted signal. Each copy will be delayed by the propagation time required to travel the path length to/from its respective the multi-path reflector. The reception of both the direct-path signal and the several multi-path signals is illustrated in Figure 4.
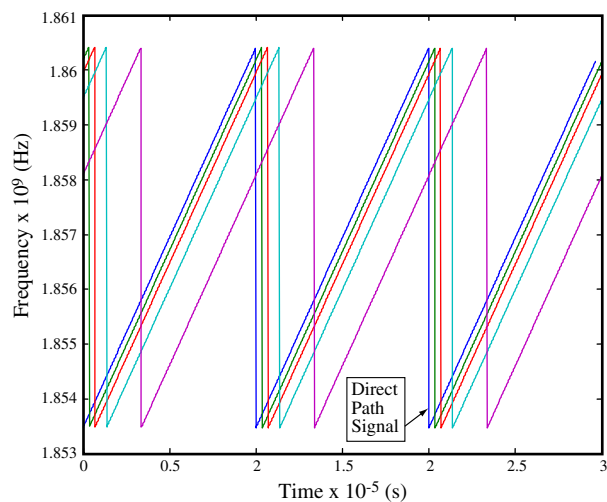
Figure 4: Power spectral density of the received signals. The first signal to arrive is the direct-path signal and the others are the delayed multi-path signals.

The composite signal received at the antenna is combined with the internal reference signal in the signal mixer, which effectively multiplies the received signals, both the direct-path and the n-multi-path delayed copies, with the reference copy of the transmitted signal. At any point in time, the internal reference copy of the transmitted signal is at a higher frequency than the delayed received signals. This is due to the longer delay in the propagation of the signals during transmission through free space than the internal reference, which is transmitted internally over a very short segment of coaxial cable or micro-strip circuit board trace. The signal multiplication properties of the mixer calculate the sum and difference of these two frequencies, as detailed in Eqs. 7 through 11. Fol-

lowing the mixer, the sum and difference signals are passed through a low pass analog filter, which removes the upper side-band portion of the signals and leaves only the difference signals in the captured waveform. The conceptual theoretical difference frequency for the direct path signal and delayed multi-path signals is shown in Figure 5. This figure demonstrates that the direct path signal is the lowest frequency component of the combined signal, because it takes the shortest path to the receiving antenna. The direct path signal is the closest in time, and therefore, frequency to the internal reference copy of the swept frequency transmitted signal. While this theoretical conception provides insight, transforming the time-based signal along with multiple delayed copies into the frequency domain by means of a fast Fourier transformation shows the expected true phenomena. The technique first subtracts the mean from the signal to remove the DC component and then uses a Hanning window to provide good spectral separation (Pozar, 1998; Strum and Kirk, 1988) before performing the discrete Fourier transformation. The complex Fourier transformed data is then multiplied by its complex conjugate to form the power spectral density, which allows for visualization of the location of the energy of the direct-path and the multi-path signals within the frequency domain.
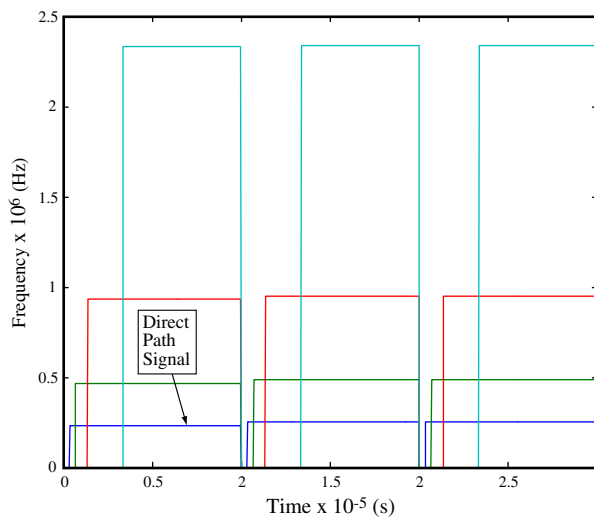

Figure 5: Theoretical plot of frequency versus time of the received signals after mixing to heterodyne the signals to lower frequency. The smallest frequency signal corresponds to the direct path signal and the others are the delayed multi-path signals.

For investigation of the proposed system, a direct-path transmitted signal (1 m delay) was combined with three time-delayed multi-path copies (3, 5, 20 m delays). These signals were then heterodyned

down to the base-band as they would be in practice by the signal mixer [the down-conversion process, which is performed by multiplying by the internal reference copy (0 meter delay) to the direct-path delayed signal and summed with the further delayed multi-path signals]. After mixing, an image-rejection filtering operation is performed by digitally low-pass filtering to remove the upper side-band images. In practice, this step would be performed by an analog low-pass filter to avoid aliasing, because the upper-band components are beyond the capabilities of today's analog to digital converters. Since this was not an option for the simulation, aliasing in the simulation was avoided by over-sampling, low-pass filtering, and signal decimation. Taking the output from the image rejection step, the power spectral density was calculated to determine the location of the energy of the direct-path, as well as the delayed multi-path signals, because they would be received after the mixing and image-rejection filtering step, thereby providing the signal as it would be digitized by the system in practice. Figure 6 details all of the direct-path plus multi-path signals after down-converting and image-rejection filtering.
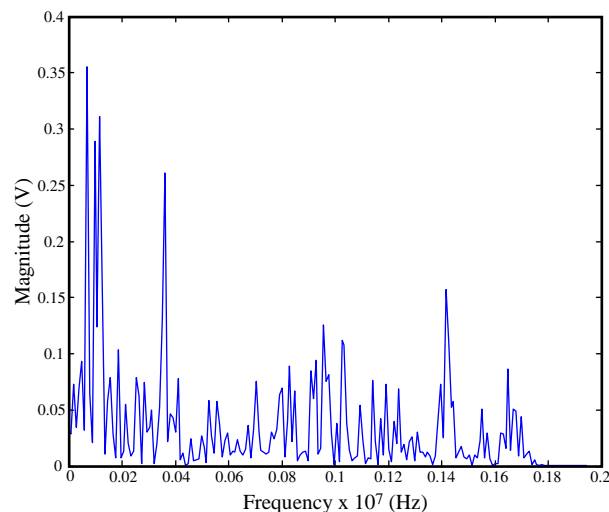

Figure 6: Power spectral density of the received signals after mixing and image rejection filtering (includes both the direct path plus all of the multi-path components).

RESULTS

Insight can be gained by examining separately all of the received components in the frequency domain. Figure 7 shows the direct-path only signal, as analyzed according to the signals in Figure 6,

and Figures 8 through 10 detail each of the received multi-path components that were received separately, again as analyzed according to Figure 6. By looking at each signal component separately, the location of the energy from each component in the frequency domain becomes clear. It is also of interest that the more delayed the signal, the greater the spread in the frequency of the signal. In the process of spreading the signal, the magnitude of the signal strength is lowered as the total energy is spread across a much larger frequency window. This is advantageous, because it is naturally providing some filtering to the unwanted multi-path components. This analysis reveals that the direct-path component is distinctly separated within the frequency domain from the other multi-path components, so the direct-path signal can be isolated from the multi-path components through a standard filtering process if a very sharp cut-off filter is applied to the data. Using the multi-path occupied frequencies as detailed in Figures 7 through 10, an elliptic 8th order low pass filter (Fig. 11) was designed to remove all multi-path components from the combined received signal. After application of the digital low-pass filter (Fig. 11) to the all of the combined signals, as noted in Figure 6, it can be seen in Figure 12 that the direct-path component has been significantly raised above the out-of-band noise. Analysis of the magnitude of the out-of-band noise to the desire direct-path signal produced a 37 dB signal to noise improvement over the unfiltered case.
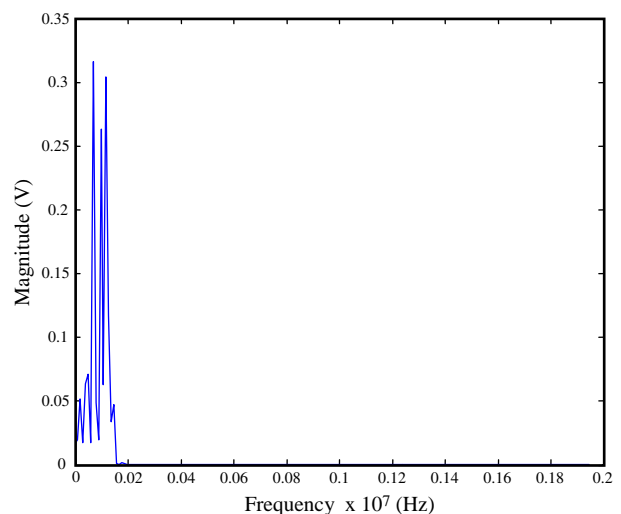

Figure 7: Power spectral density of the direct-path signal after mixing and image rejection filtering. The Fourier transformation was performed after mixing the signal down to the base-band frequency.
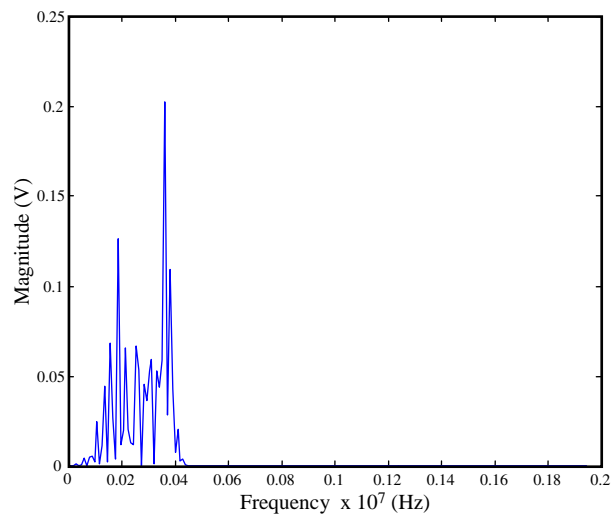
Figure 8: Power spectral density of the first multi-path signal to arrive at the receiving antenna after mixing and image rejection filtering. The Fourier transformation was performed after mixing the signal to the base-band frequency.
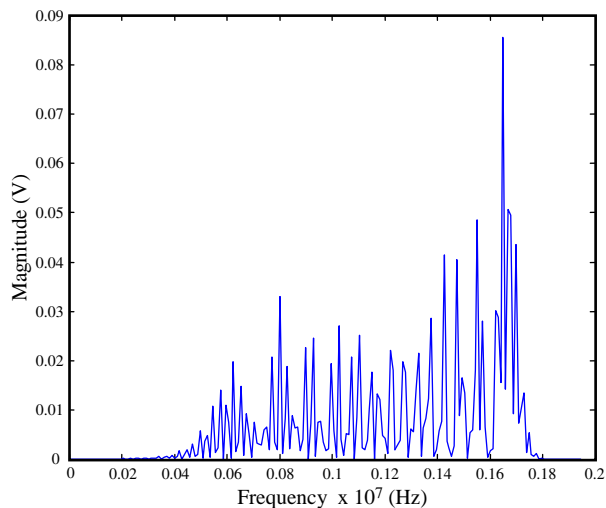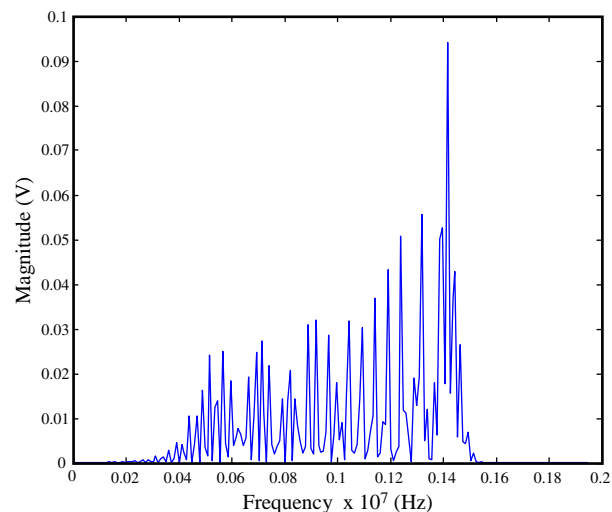

Figure 10: Power spectral density of the third multi-path signal to arrive at the receiving antenna after mixing and image rejection filtering. The Fourier transformation was performed after mixing the signal to the base-band frequency.

Figure 9: Power spectral density of the second multi-path signal to arrive at the receiving antenna after mixing and image rejection filtering. The Fourier transformation was performed after mixing the signal to the base-band frequency.
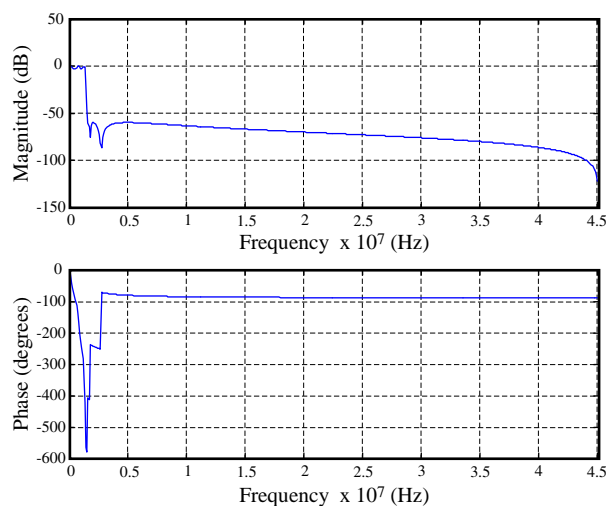

Figure 11: Digital low-pass filter used to separate the direct-path signal from the propagation delayed multi-path components.

Once the target band-pass window was identified, a low-pass or band-pass filter centered about that frequency provides a means to remove the multi-path components. Using the previously described techniques, the system with the addition of the three multi-path interferers after mixing produced a time domain signal as shown in Figure 13. After applying,

the previously described digital low-pass, multi-path rejection filter to the signal, the direct-path signal was recovered and is shown in Figure 14. As is shown, the system can then measure the average frequency of this recovered signal to provide a measure of the permittivity of the material.
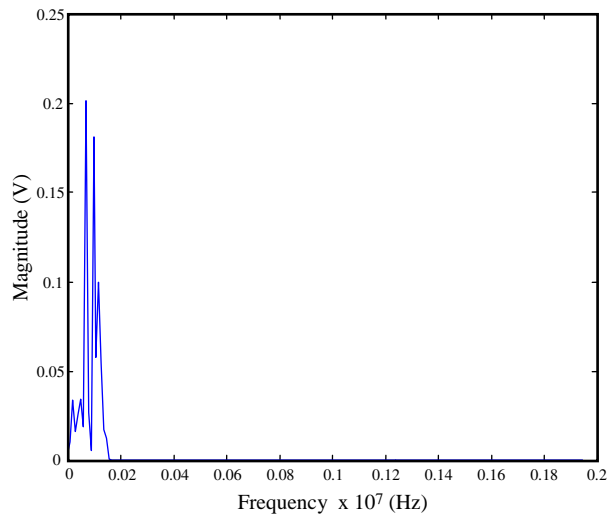
Figure 12: Power spectral density of all of the received signals (direct and all multi-path signals) that arrive at the receiving antenna after mixing, image rejection filtering, and digital low pass filtering using filter of Figure 11.
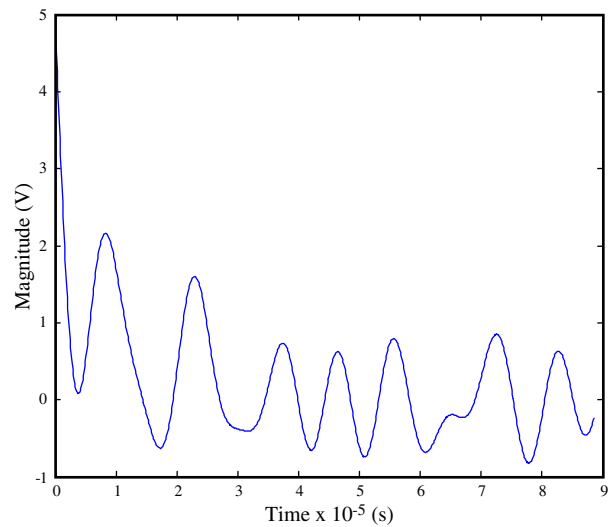

Figure 14: Time domain plot of all of the received signals (direct and all multi-path signals) that arrive at the receiving antenna after mixing, image rejection filtering, and digital low pass filtering using filter of Figure 11.
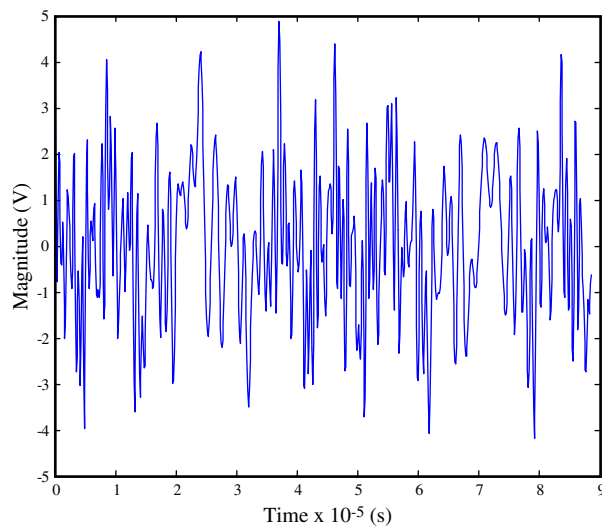

Figure 13: Time domain plot of all of the received signals (direct and all multi-path signals) that arrive at the receiving antenna after mixing and image rejection filtering.

Since the proposed design cannot infinitely ramp the frequency upward, at some point the system has to repeat and start over and repeat. This feature causes the system to start over at some future delta-*t*, when it does, it is possible that a long multi-path signal will also arrive at this time. This leads to an ambiguity between the direct path and this long multi-path signal. The length of this long multi-path component can be calculated by the frequency of the repetition rate as $t = 1/f$ (frequency$_{repetition}$), which gives the path length of the ambiguity distance [c (speed of light)/f]. For this system, this distance occurs at 28 m. To minimize this effect, a band-pass filter is a better option than the low-pass filter used in this analysis. Alternatively, to remove the effect of the folded in multi-path components, the signal measurement can be repeated over a different frequency modulation range where that specific ambiguity multi-path signal will appear in a different portion of the frequency domain and will thereby be removed. In this way, the system can also remove the folded-in multi-path signals from the direct-path signal.

In summary, the proposed system will, after the mixing process, filter the signal with a low order analog image-rejection filter, then digitize the signal and process it again with a high-order digital low-pass or band-pass filter that is designed to pass (preserve) only the frequencies where the direct path signal is located. This removes all of the other undesired components of the signal, such as the multi-path components, that lie outside this narrow frequency window. The advantage of performing the filtering in two separate stages is that the analog image rejection/anti-aliasing filter can be a low order filter where temperature drift is tolerable, which can then be followed by a high-order digital filter. This provides the ability to tighten the frequency window width around the desired signal component without regard to component tolerances and temperature effects, which leads to a much narrower window and enhanced multi-path signal rejection.

CONCLUSIONS

If a continuously swept microwave frequency is used as the energy probe for measuring cotton bale moisture, it should provide a robust measurement of the moisture content of the cotton bale with a high degree of multi-path rejection capability. The system was shown to perform well with multi-path reflectors as close as 2 m. With sufficient care in the placement of the device inside a cotton gin, this type of system should be installed so that most of the metallic reflectors are at least 2-3 m away. Given this assumption, the expected signal to noise rejection of the direct path signal to the multi-path signals should exceed 40 dB. At this level, the measurement should be largely unaffected by the spurious emissions, so that the system is robust and will not require field calibration. It should also be noted that due to the small radar cross-section of the cotton bale ties, spurious reflections are not expected to impact the measurement. Other confounding issues, such as temperature and surface moisture, will need to be explored in future research.

The simulations of this research indicate that this modulation technique should be able to provide a system that is highly tolerant of multi-path interference while preserving the permittivity information contained within the transmitted microwave signal that is used in the microwave moisture sensing process. Given these promising results, future research will be conducted to investigate potential hardware designs to realize these techniques.

REFERENCES

Balanis, C.A. 1982. Antenna theory, analysis and design. Harper & Row, New York, N.Y.

Cheng, D.K. 1992. Field and wave electromagnetics. 2nd ed., Addison-Wesley Publishing Co., Reading, MA.

Kraszewski, A.W., S. Trabelsi, and S.O. Nelson. 1996. Wheat permittivity measurements in free space. J. Microwave Power Electromagnetic Energy 31(3):135-141.

Kraszewski, A.W. 1988. Microwave monitoring of moisture content in grain-further considerations. J. Microwave Power Electromagnetic Energy 23(4):236-246.

Lee, J.S., and L.E. Miller. 1998. CDMA systems engineering handbook. Artech House, Boston, MA.

Nelson, S.O., A.W. Kraszewski, S. Trabelsi, and K.C. Lawrence. 2000. Using cereal grain permittivity for sensing moisture content. IEEE Trans. Instrumentation Measurement 49(3):470-475.

Peebles, P.Z., Jr. 1998. Radar principles. John Wiley and Sons, Inc., New York, N.Y.

Pelletier, M.G. 2004. Multipath interference investigation for cotton bale microwave moisture sensing. J. Cotton Sci. 8(3):170-178 [Online]. Available at http://www.cotton. org/journal/2004-08/3/170.cfm.

Pozar, D.M. 1998. Microwave engineering, 2nd ed., Wiley, New York, N.Y.

Strum, R.D., and D.E. Kirk. 1988. First principles of discrete systems and digital signal processing. Addison-Wesley Publishing Co. Reading, MA.

Sremler, F.G.. 1992. Introduction to communication systems, 3rd ed., Addison-Wesley Publishing Co. Reading, MA.

Trabelsi, S., A.W. Kraszewski, and S.O. Nelson. 2001. New calibration technique for microwave moisture sensors. IEEE Trans. Instrumentation Measurement 50(4):877-881.